RSC Advances

Volume 1 | Number 1 | Jan 2013 | Pages 1–100

RSC Advances

www.rsc.org/advances

ROYAL SOCIETY OF CHEMISTRY

ROYAL SOCIETY OF CHEMISTRY

www.rsc.org/advances

Solution processable polyamines via click chemistry for water purification

Vanga Devendar Goud, Roshan DSouza, Suresh Valiyaveettil*

Abstract: Amine functionalised polymers are not widely used in applications owing to increased reactivity, sensitivity to air and moisture, low stability and processing difficulties. Here, we report a convergent strategy for the synthesis of four stable and processable amphiphilic amine functionalized poly(N-triazolepropyl phenyl aniline-*co*-styrene) **P1**, poly(N-triazoleoctyl phenyl aniline -*co*-styrene) **P2**, poly(N-triazolexylyl phenyl aniline-*co*-styrene) **P3**, and poly(N-aminopropylphenyl pyridine-*co*-styrene) **P4**, using click reaction. Full structural characterization and properties of the polymers are established using different spectroscopic and physicochemical methods. All polymers were soluble in common organic solvents and insoluble in water. Porous films and spherical particles were obtained via drop-casting the solutions of copolymers in chloroform or in *N*,*N*-dimethylformamide, respectively, on glass substrates. The synthesized polyamines were used for the liquid-liquid and solid-liquid extraction of metal nanoparticles, organic dyes and heavy metal ions from water. All polymers showed significant extraction efficiencies towards metal nanoparticles (20 – 45 mg/g) and organic dyes (25 – 70 mg/g) dissolved in water. Such synthetic polyamines can be used as potential adsorbents for water purification.

Keywords. Polyamine; Polystyrene, Free radical polymerization; Click reaction; 1,2,3-Triazole; Self-assembly; Organic dyes; Heavy metal ions; Kinetics

Introduction

Nanoparticles are widely used in consumer products such as cosmetics, cleaning agents, clothing and washing machines.[1] The increased use of nanoparticles in various commercial products enhances the possibility for contamination of environment.[2,3] Since ultra-small metal particles Are known to cause health risks for living systems,[4-9] it is important to remove them from contaminated water. However, the direct separation is difficult owing to their small size, high reactivity and large surface area of nanoparticles. This warrants the development of new materials and methods for water purification in the near future.

Synthesis of polyamines has attracted significant interests in recent years owing to their sensitivity towards changes in pH, high reactivity and toxicity in living organisms.[10-14] Polyamines are used to extract heavy metal ions, nanoparticles and organic pollutants through electrostatic interactions.[15-22] Polyethylenimine (PEI) with large number of primary and secondary amino groups exhibits good sorption ability for heavy metals.[23,24] 1,2,3-Triazole group, a versatile functional heterocycle unit formed by click reaction, has been used in supramolecular chemistry for coordination with anionic, neutral and cationic guest molecules.[25] Recently, we reported the synthesis and characterization of polyamines for the removal of dissolved metallic nanoparticles from water.[26]

A few challenges related to polyamines are addressed in this paper, which include stability, easy accessibility, processability and proof of concept demonstration of potential use as adsorbent for water purification. Here we report a simple method for the synthesis of amphiphilic polyamines using click reaction and investigate potential application in liquid - liquid and solid – liquid extraction for the removal of dissolved pollutants from water. The choice of polystyrene as a backbone was based on synthetic flexibility and potential for introducing different amine functional groups towards enhancing the extraction efficiencies. The target polymers are designed in such a way that the substituted aniline and pyridine incorporated side chains are connected to the polymer backbone through a flexible spacer. Alkyl chain spacer provides flexibility for the amine groups to interact with various pollutants. In addition the incorporation of 1,4-substituted benzene in the side chain, makes the polymer P3 more rigid as compared to other polymers. The concept and the target polymers are shown in Figure 1.

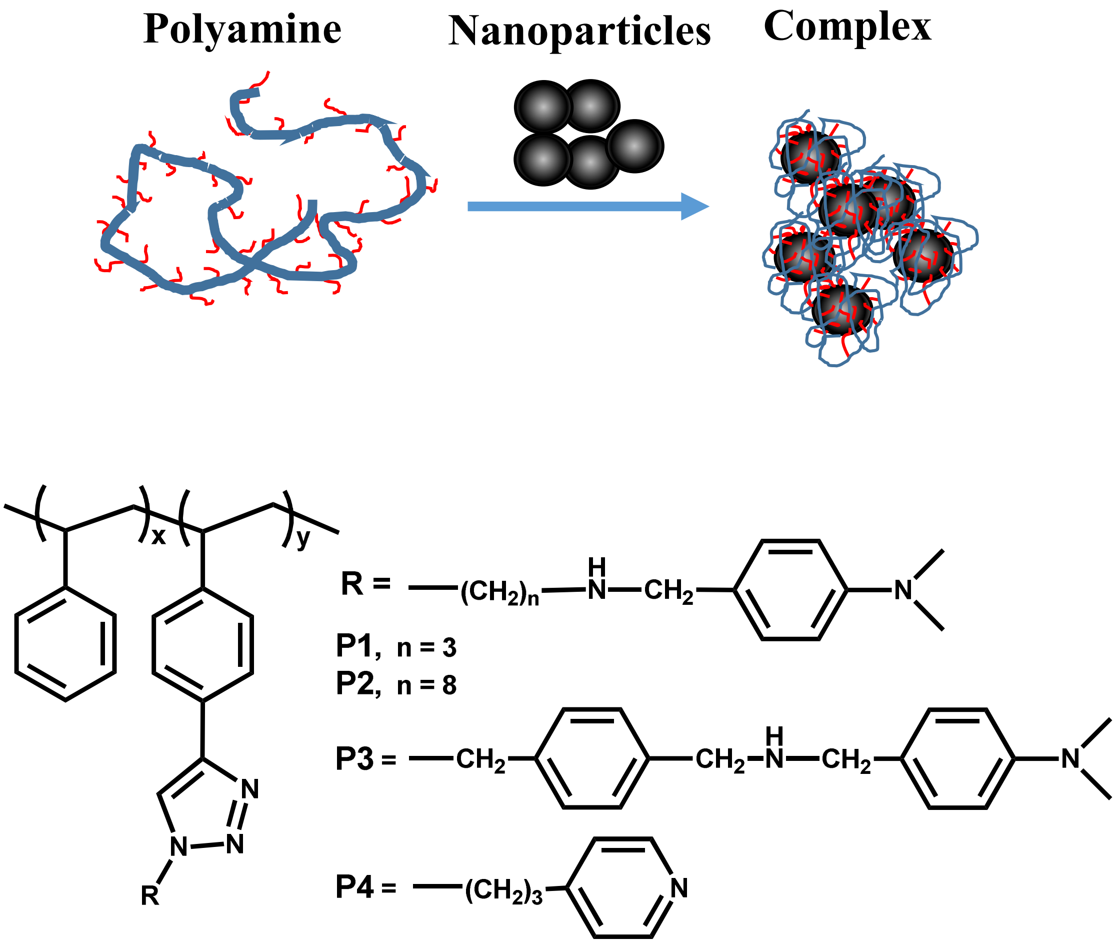

Fig. 1 Schematic representation of the binding of nanoparticles with amine functionalized polymer and the molecular structure of random copolymers **P1** – **P4**.

Experimental

Materials

Styrene (99%), 4-bromo styrene (98%), silver nitrate ($AgNO_3$), sodium citrate, hydrogen tetrachloroaurate trihydrate ($HAuCl_4•3H_2O$), azobisisobutyronitrile (AIBN), diisopropylethylamine (DIPEA), bromotris(triphenylphosphine)copper(I) ($CuBr(PPh_3)_3$), sodium borohydride ($NaBH_4$) and HPLC grade solvents where purchased from commercial sources. All materials were used without further purification, unless specified otherwise. Chloroform ($CHCl_3$) and *N*,*N*-dimethylformamide (DMF) were used for processing polyamines. Polyvinylpyrrolidone (PVP) capped water soluble Au and Ag nanoparticles were prepared according to reported procedures.[27] Deionised water was used for preparing stock solutions of nanoparticles.

Measurements

Gel permeation chromatography (GPC) for polymers was performed on Waters e2695 alliance system equipped with Waters 2414 refractive index detector using THF as the eluent, flow rate of 0.3 mL/min at 40 °C and polystyrene standards for calibration. ^1H and ^{13}C nuclear magnetic resonance (NMR) spectra were recorded on Bruker Avance AV300 (300 MHz) NMR instrument using $CDCl_3$ as the solvent. Bruker ALPHA FT-IR spectrophotometer was used for recording FT-IR spectra of polymers. Thermogravimetric analyses (TGA) were conducted using a SDT 2960 TA instrument. All samples were heated under nitrogen atmosphere from 25 to 800 °C using a heating rate of 10 °C/min. Differential scanning calorimetry (DSC) measurements were done under nitrogen atmosphere using a Mettler Toledo DSC1 STARe System. Scanning electron microscope (SEM) images for random copolymers were taken with a field emission scanning electron microscopy (FESEM; JEOL JSM-6701F). The samples were mounted on copper stubs with double-sided conducting carbon tape and sputter-coated with platinum (2 nm) before examination. The size of the nanoparticles was determined using a transmission electron microscope (TEM, JEOL JEM 2010). The extraction efficiency of polymers was quantified using a UV-Vis spectrophotometer (Shimadzu-1601 PC spectrophotometer).

General procedure for click reaction

A solution of the polymer (1.0 eq., based on (trimethylsilyl)ethynylstyrene units) in THF (20 mL) was treated with azide derivatives (1.0 eq.), $CuBr(PPh_3)_3$ (0.01 eq.), and diisopropylethylamine (DIPEA, 0.5 mL, excess), and the mixture was allowed to stir at room temperature for 24 h. After removing the solvent under reduced pressure, the crude polymer was precipitated in excess methanol. The solid was filtered, washed repeatedly with methanol and dried under high vacuum at 40 °C for 16 h.

Synthesis of monomer 2:[28-32]

To a solution of 4-bromostyrene **1** (5 g, 27.5 mmol) in dry triethylamine (100 mL) was added trimethylsilylacetylene (6.0 g, 60.4 mmol) and bis(triphenylphosphine)palladium(II) chloride (0.38 g, 0.55 mmol). The reaction mixture was heated to 50 °C for five minutes and copper(I) iodide (0.06 g, 0.41 mmol) was added. The color of the solution changed from red to dark brown. The mixture was stirred for an additional 16 hours at 50 °C and the precipitated triethylammonium salt was removed by filtration and the excess solvent in the filtrate was removed under reduced pressure. The obtained brown crude compound was purified over column chromatography eluting with n-hexane to yield compound **2** as a colorless liquid (3.55 g, 65%). ^{1}H NMR: δ 7.43 (d, J = 8.0 Hz, 2H), 7.34 (d, J = 8.0 Hz, 2H), 6.69 (dd, J = 11.2, 17.6 Hz, 1H), 5.75 (d, J = 17.6 Hz, 1H), 5.28 (d, J = 11.2 Hz, 1H), 0.26 (s, 9H). ^{13}C NMR: δ 137.59, 136.19, 132.13, 125.99, 122.35, 114.82, 105.07, 94.80, -0.03.

Synthesis of homopolymer 3:

A mixture of (trimethylsilyl)ethynylstyrene **2** (0.5 g, 2.5 mmol) and AIBN (0.004 g, 0.01 eq.) in dry THF (5 mL) was degassed by repeated freeze-pump-thaw cycles, sealed under vacuum and heated at 70 °C for 4 hours. The viscous reaction mixture was dissolved in THF (5 mL) and precipitated in excess methanol to give crude polymer which was treated with tetrabutylammonium fluoride (5 mL, 1 M in THF, 2 eq.) to remove trimethylsilyl groups, stirred for two hours at 0 °C and concentrated under reduced pressure. The crude polymer was precipitated three times in methanol to afford **3** as a white powder (0.35 g, 70 %, M_n = 7540 g/mol, PDI = 1.7); ^{1}H NMR (300 MHz, $CDCl_3$): δ 7.24-6.93 (m, Ar-H), 6.78-6.25 (m, Ar-H), 1.90-1.23 (m, $-CH_2-CH-$), 0.36-0.24 (s, $Si(CH_3)_3$); IR (KBr, cm^{-1}): 3025 (Ar-H), 2930 (C-H), 2145 ($-C\equiv C-$), 1620 ($-C=C-$).

Synthesis of homopolymer 4:

Click reaction of polymer **3** (0.3 g) with azide derivative **8** (0.3 g, 1.27 mmol) in presence of $CuBr(PPh_3)_3$ (0.04 g, 0.01 eq.) and DIPEA (0.5 mL) afforded homo-polymer **4** in quantitative yield; IR (KBr, cm^{-1}): 3445(N-H), 3021 (Ar-H), 2935 (C-H), 1605 ($-C=C-$).

Synthesis of poly[styrene-*r*-(trimethylsilyl)ethynylstyrene] 6:

A mixture of styrene **5** (6.0 g, 57.6 mmol, 5 eq.) and (trimethylsilyl)ethynylstyrene **2** (2.3 g, 11.5 mmol, 1 eq.) in dry THF (5 mL) was added AIBN (0.01 g, 0.01 eq.) and degassed by repeated freeze-pump-thaw cycles, sealed under vacuum and heated at 70 °C for 12 hours. The viscous reaction mixture was dissolved in THF (5 mL) and precipitated in excess methanol to give polymer **6** as a white powder (6.5 g, 81 %, M_n = 37056 g/mol, PDI = 2.2); ^{1}H NMR (300 MHz, $CDCl_3$): δ 7.25-6.95 (m, Ar-H), 6.75-6.22 (m, Ar-H), 1.95-1.25 (m, $-CH_2-CH-$), 0.37-0.27 (s, $Si(CH_3)_3$); IR (KBr, cm^{-1}): 3023 (Ar-H), 2915 (C-H), 2150 ($-C\equiv C-$), 1596 ($-C=C-$).

Synthesis of poly[styrene-*r*-4-ethynylstyrene] 7:

To a solution of poly(styrene-*co*-trimethylsilylethynylstyrene) **6** (5.0 g, 0.81 mmol based on (trimethylsilyl)ethynylstyrene units) in dry THF (100 mL), tetrabutylammonium fluoride (1.6 mL, 1 M in THF, 2 eq.) was added and stirred for two hours at 0 °C. The solution was concentrated under reduced pressure and the polymer was precipitated three times in methanol to give **7** as a white powder (Yield: 90%, M_n = 28400 g/mol, polydispersity index (PDI) = 1.8); ^1H NMR (300 MHz, $CDCl_3$): δ 7.25-6.95 (m, Ar-H), 6.75-6.30 (m, Ar-H), 3.12-3.03 (s, $-C{\equiv}C-$), 1.96-1.26 (m, $-CH_2-CH-$); IR (KBr, cm^{-1}): 3025 (Ar-H), 2928 (C-H), 2155 ($-C{\equiv}C-$), 1610 ($-C{=}C-$).

Synthesis of polymer P-1:

Click reaction of poly[styrene-*r*-4-ethynylstyrene] **7** (1.0 g) with azide derivative **8** (0.3 g, 1.27 mmol) in presence of $CuBr(PPh_3)_3$ (0.04 g, 0.01 eq.) and DIPEA (0.5 mL) afforded **P-1** in quantitative yield; ^1H NMR (300 MHz, $CDCl_3$): δ 7.24-6.88 (m, Ar-H), 6.74-6.27 (m, Ar-H), 4.54-4.40 (m, triazole-CH_2), 3.70-3.64 (s, Ar-CH_2), 2.95-2.85 (s, $N(CH_3)_2$), 2.70-2.60 (m, N-CH_2), 2.15-1.25 (m, $-CH_2-CH-$); IR (KBr, cm^{-1}): 3440 (N-H), 3021 (Ar-H), 2926 (C-H), 1601 ($-C{=}C-$).

Synthesis of polymer P-2:

Click reaction of poly[styrene-*co*-4-ethynylstyrene] **7** (1.0 g) with azide derivative **9** (0.38 g, 1.27 mmol) in presence of $CuBr(PPh_3)_3$ (0.04 g, 0.01 eq.) and DIPEA (0.5 mL) afforded **P-2** in quantitative yield; ^1H NMR (300 MHz, $CDCl_3$): δ 7.22-6.85 (m, Ar-H), 6.75-6.28 (m, Ar-H), 4.40-4.30 (m, triazole-CH_2), 3.72-3.62 (s, Ar-CH_2), 2.97-2.85 (s, $N(CH_3)_2$), 2.65-2.55 (m, N-CH_2), 2.00-1.20 (m, $-CH_2-CH-$); IR (KBr, cm^{-1}): 3410 (N-H), 3023 (Ar-H), 2930 (C-H), 1618 ($-C{=}C-$).

Synthesis of polymer P-3:

Click reaction of poly[styrene-*co*-4-ethynylstyrene] **7** (1.0 g) with azide derivative **10** (0.37 g, 1.27 mmol) in presence of $CuBr(PPh_3)_3$ (0.04 g, 0.01 eq.) and DIPEA (0.5 mL), afforded **P-3** in quantitative yield; ^1H NMR (300 MHz, $CDCl_3$): δ 7.25-6.88 (m, Ar-H), 6.80-6.35 (m, Ar-H), 5.60-5.45 (m, triazole-CH_2), 3.88-3.77 (s, Ar-CH_2), 3.77-3.67 (m, N-CH_2), 2.97-2.87 (s, $N(CH_3)_2$), 1.95-1.25 (m, -CH_2-CH-); IR (KBr, cm^{-1}): 3420 (N-H), 3024 (Ar-H), 2926 (C-H), 1615 (—C=C—).

Synthesis of polymer P-4:

Click reaction of poly[styrene-*co*-4-ethynylstyrene] **7** (1.0 g) with azide derivative **11** (0.2 g, 1.27 mmol) in presence of $CuBr(PPh_3)_3$ (0.04 g, 0.01 eq.) and DIPEA (0.5 mL), afforded **P-4** in quantitative yield; ^1H NMR (300 MHz, $CDCl_3$): δ 7.20-6.90 (m, Ar-H), 6.75-6.35 (m, Ar-H), 4.50-4.35 (m, triazole-CH_2), 2.44-2.25 (m, Py-CH_2), 1.97-1.30 (m, -CH_2-CH-); IR (KBr, cm^{-1}): 3425 (N-H), 3027 (Ar-H), 2910 (C-H), 1592 (—C=C—).

Liquid – liquid extraction of metal nanoparticles, dyes and metal ions

A solution (400 µL) of amine-functionalized amphiphilic random copolymers (1 mg / 4 mL) in chloroform was taken in a 2 mL centrifuge tube containing aqueous solution of citrate or PVP capped Au- or Ag nanoparticle (1.5 mL, 2.5×10^{-4} M) or aqueous solutions of dyes or metal ions (1.5 mL, 100 ppm) and agitated using a mechanical shaker (200 rpm) for 6 h. All extraction experiments were performed at room temperature (25 °C) and neutral pH. The residual concentrations of nanoparticles and dyes in aqueous solution were analyzed periodically until the system reached equilibrium. For quantification, nanoparticle solutions were analysed using UV-Vis spectroscopy to estimate the amount of nanoparticles or dyes remained in the aqueous solution after extraction. The concentrations of metal ions were determined using inductively coupled plasma – optical emission spectroscopy (ICP-OES) system. The extraction capacity Q_e (mg/g) was calculated using the following equation.[33]

$$Qe = (C_0-C_e)V/M \qquad (1)$$

where C_0 and C_e (mg/L) are initial and equilibrium concentration of nanoparticles, V is the volume of the nanoparticles solution and M is mass of the adsorbent used.

Solid-liquid extraction of nanoparticles

For solid-liquid extraction, polymer solution in $CHCl_3$ (1 mg/mL) was drop cast on a glass slide to form a porous film through slow evaporation of the solvent. The morphology of the film was characterized using SEM. The glass slide with the polymer film was dipped in aqueous solution of nanoparticles (2 mL / 50 ppm) and allowed to stand at room temperature for 3 h, removed, washed with water, dried and analysed using SEM to check changes in surface characteristics before and after extraction studies.

Results and discussions

As illustrated in Scheme 1, the homopolymer **4** was synthesized from commercially available starting material, 4-bromostyrene **1** in 3 steps.[28-32] However, the final polymer was insoluble in common solvents and not characterized fully. This prompted us to copolymerize monomer **2** with styrene to develop soluble and processable polyamines (Scheme 2). A random copolymer of styrene and monomer **2** (5:1) was prepared using free radical polymerization, and removal of trimethylsilyl groups using tetrabutylammoniumfluoride (TBAF) gave the desired acetylene incorporated macromolecule **7** (Mn = 28400 amu; PDI = 1.8). From the ^{1}H-NMR spectrum, the peak integral ratio of the styrene unit and *p*-(acetylene)styrene was 5:1, which shows an approximately 227 repeating units of styrene and 36 repeating units of *p*-(acetylene)styrene in the PS-*r*-PES polymer. The acetylene groups on the polymer **7** were used for click reaction with various azide derivatives (**8** – **11)** in presence of Cu(I) and DIPEA[34-38] to synthesize the target polymers **P1** - **P4** in quantitative yield. The amount of acetylene functionalized repeating units on the polymer backbone is intentionally kept low to avoid solubility problems.

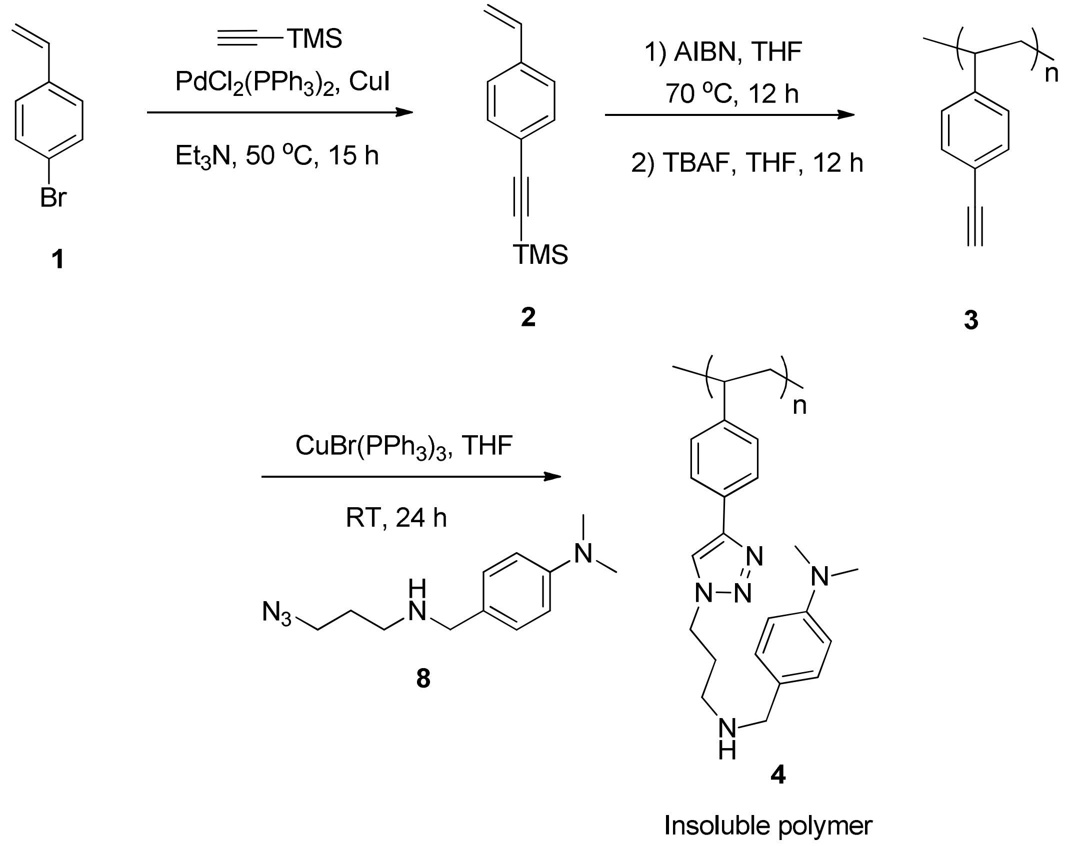

Scheme 1 Synthesis route for amine functionalized homopolymer **4**

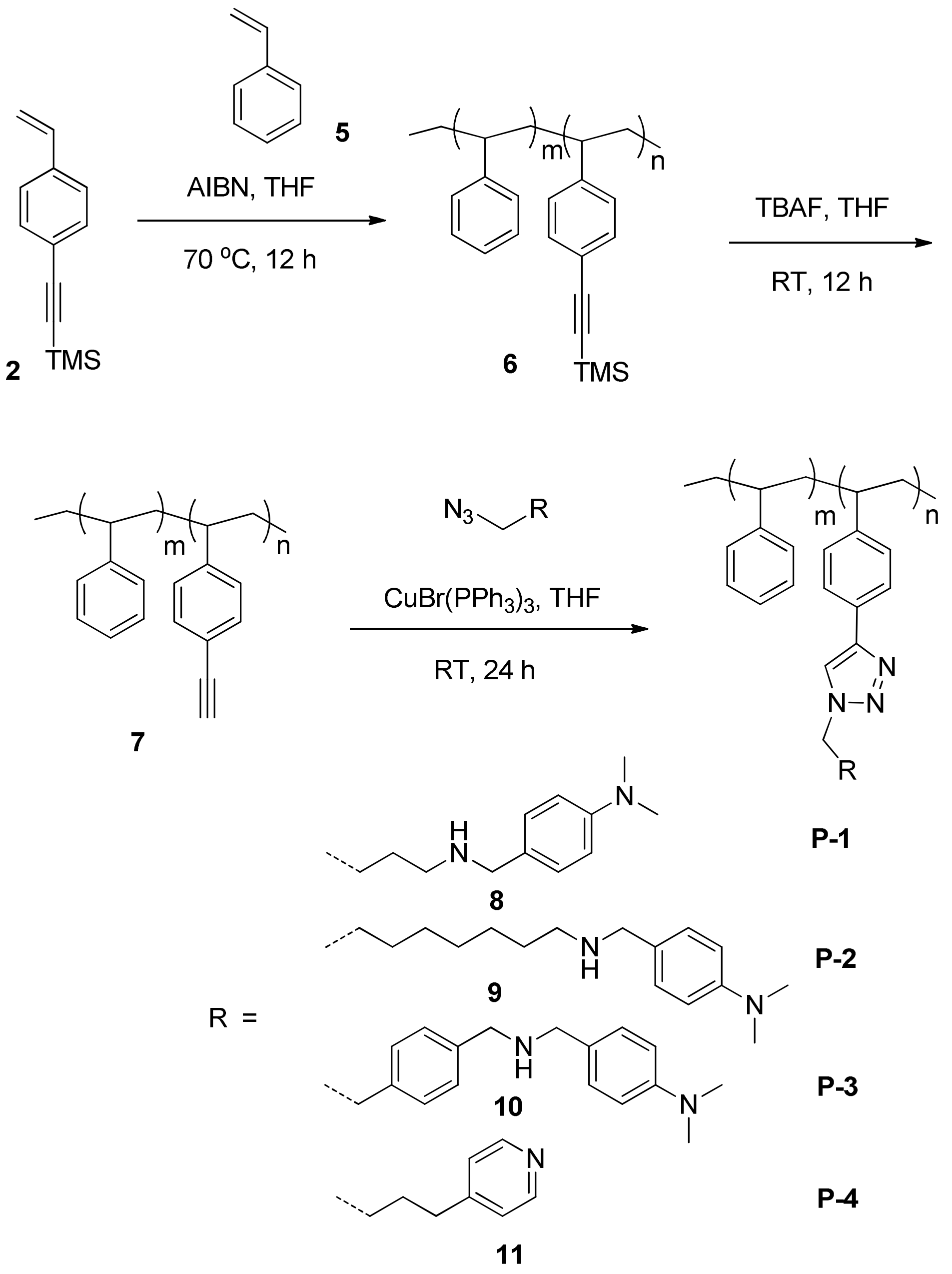

Scheme 2 Synthesis of amine functionalized copolymers **P1- P4**

Structural characterisation

The structure of target copolymers was established using ^{1}H-NMR analyses. Figure 2 shows the ^{1}H-NMR spectra for the precursor polymer, PS-*r*-PES (**7**) and all target copolymers. Conversion of the acetylene groups to the triazole moieties resulted in the appearance of new peaks at 4.54 -

4.40 ppm (m, triazole-CH_2), 2.95 ppm (s, $N(CH_3)_2$), 2.70 - 2.60 ppm (m, N-CH_2), which correspond to the formation of amines. The signal due to aliphatic protons appeared in the range from 0.9 to 2.7 ppm, whereas the alkyne proton in precursor polymer **7** showed a broad signal centered at 3.12-3.03 ppm (s, $-C\equiv C-$H), [Fig. 2 (**7**)]. The signals of aromatic protons for all polymers appeared at 7.25 - 6.30 ppm. In addition, the disappearance of the peaks due to alkyne proton centered at 3.12 - 3.03 ppm (Fig. 2, **P1-P4**) implies a quantitative conversion to triazole group during the click reaction.

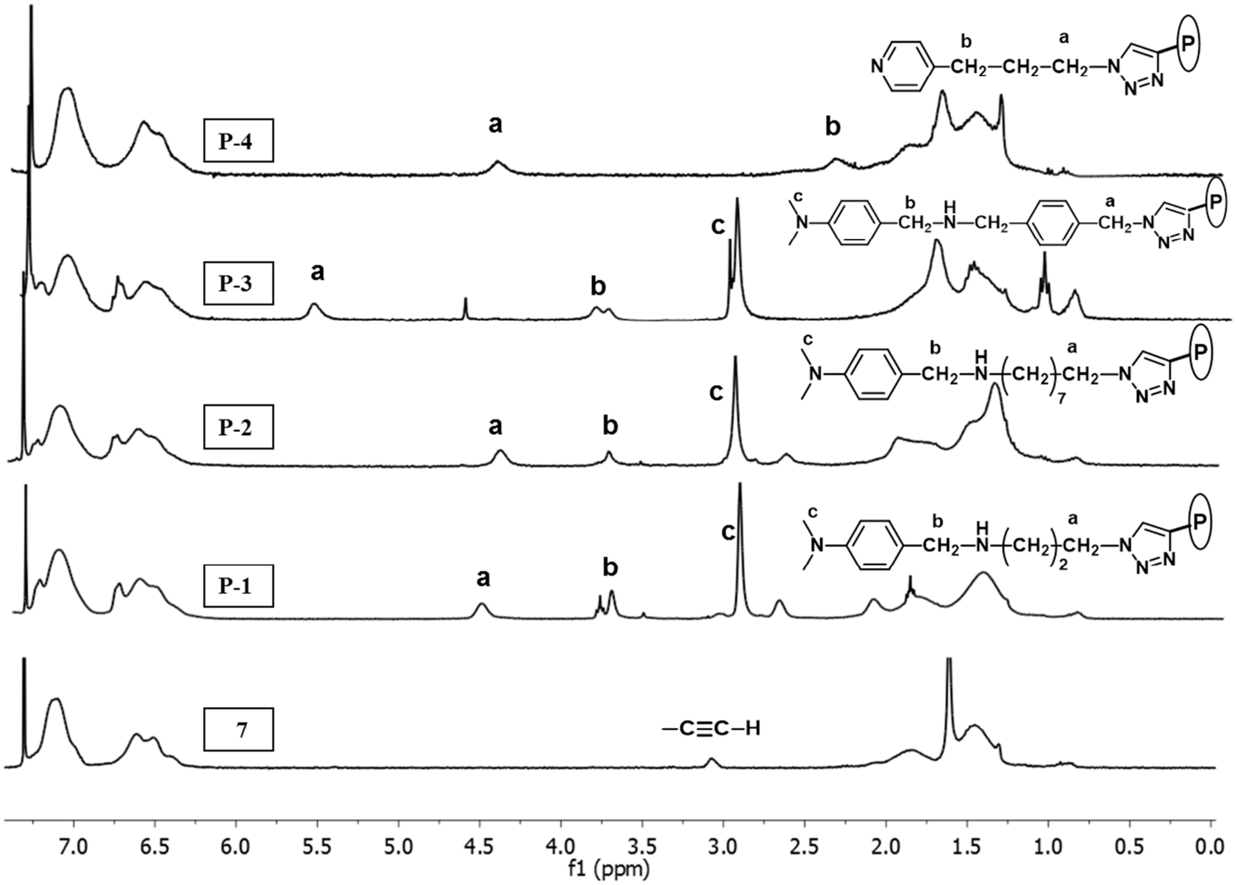

Fig. 2 ^{1}H NMR spectra of copolymers PS-*r*-PES (**7**), **P1 – P4** in $CDCl_3$ under ambient conditions

FT-IR analysis

FT-IR spectra of the polymers are shown in Figure 3. In Figure 3(a), the characteristic alkyne stretching of the precursor polymer **7** appeared at 2155 cm^{-1}. The other peaks observed at 3025, 2928, and 1610 are associated with stretching vibrations of Ar-H, C-H, and (—C=C—) bonds, respectively. After Click reaction, new peaks of the polyamines emerged in the spectrum at 3100 cm^{-1} - 3450 cm^{-1} (N-H). The peaks observed at 1590 - 1620 cm^{-1} are assigned to stretching vibrations of aromatic C-C bond. The click reaction product was further confirmed by the disappearance of 2155 cm^{-1} peak, which corresponds to —C≡C—H group.

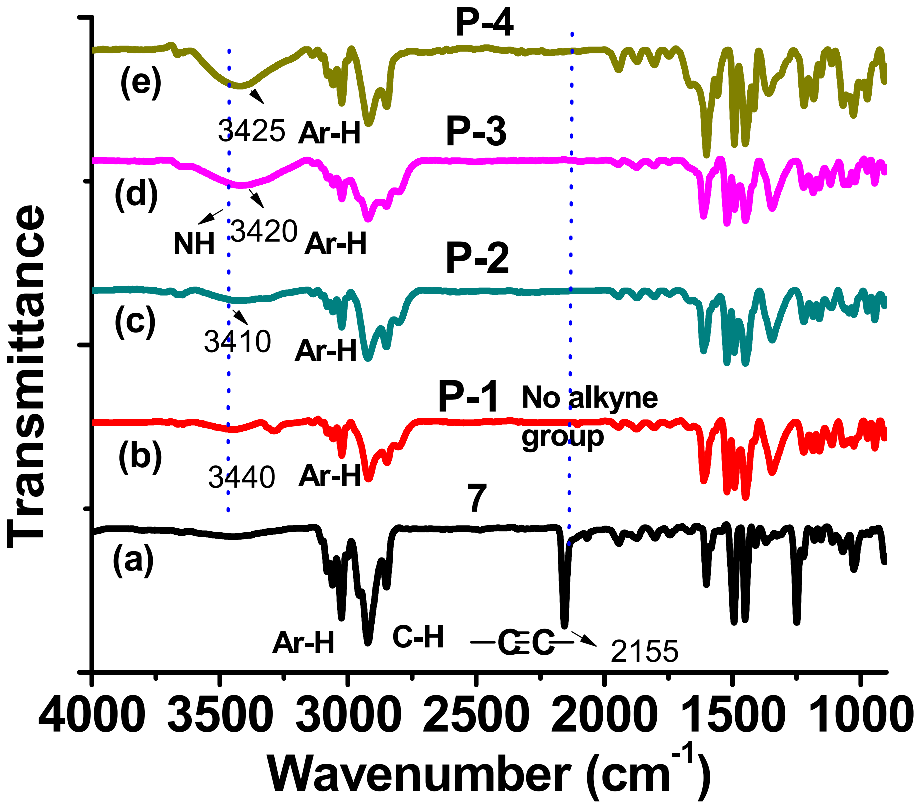

Fig. 3 FTIR spectra of precursor polymer **7** and target amine-functionalized copolymers **P1 – P4** recorded using KBr as matrix.

Thermal properties

To understand the thermal stability of the amphiphilic copolymers, thermogravimetric analysis (TGA) and differential scanning calorimetry (DSC) were performed under nitrogen atmosphere. TGA curves of all copolymers are shown in Figure 4, which suggest comparable thermal stabilities for all four copolymers. The data revealed that the polymers were stable up to 270 − 300 °C, and 50 % weight loss was observed at around 400 − 425 °C. Except **P3**, all other polymers showed single stage decomposition and a char yield at 500 °C was in the range of 10 % − 15 %. The glass transition temperatures (T_g) observed for **P1** – **P4** in the DSC analyses indicate an increasing stiffness in the copolymers with the introduction of triazole and amine groups, when compared to the precursor copolymer PS-*r*-PES (**7**). The T_g of precursor polymer **7** and polymers **P1** – **P4** are 69.9 °C, 79.2 °C, 79.3 °C, 102 °C and 110 °C, respectively (Table 1). All DSC traces are shown in supplementary information Figure S1.

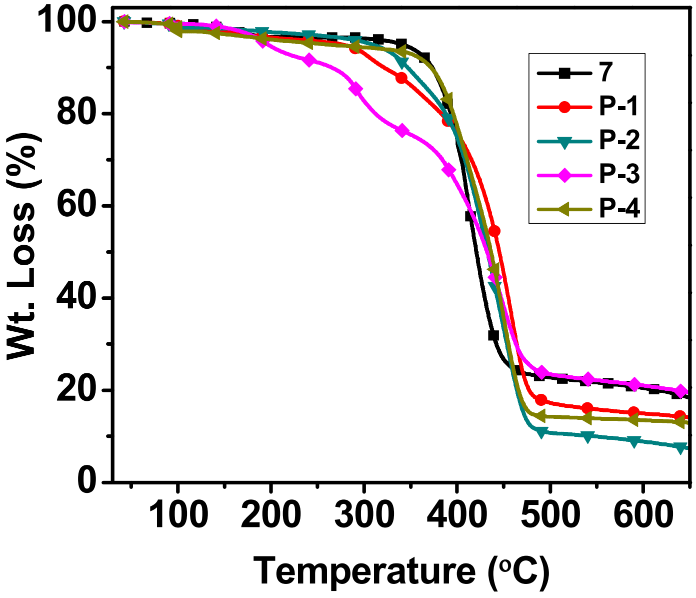

Fig. 4 TGA curves of PS-*r*-PES (7), **P1** – **P4** copolymers recorded under nitrogen atmosphere.

Table 1: Degradation temperature and T_g of precursor polymer and polymers **P1 – P4**

Polymers	**Decomposition temperature[a] (°C)**	**Glass transition temperature T_g (°C)**
PS-*r*-PES (7)	**370**	**69.9**
P1	**315**	**79.2**
P2	**345**	**79.3**
P3	**265**	**102**
P4	**368**	**110**

[a] Decomposition temperature was measured at 10% weight loss of polymers

Solubility of the polymers: Solubility depends on the structure of polymers. Polyamines are soluble in water, but insoluble in common organic solvents. The synthetic strategy reported here is used to prepare a series of amine functionalized copolymers, which are soluble in most common organic solvents such as $CHCl_3$, tetrahydrofuran, DMF and not soluble in water. The number of amine functional groups on the polymer backbone is critical to achieve the desired solubility. Homopolyamine prepared through the click reactions using acetylene functionalized polystyrene and corresponding azides was not soluble in water or organic solvents. An optimum quantities of styrene and amine functionalized styrene on the polymer backbone is important to achieve the desired solubility.

Liquid – liquid extraction of metal nanoparticles from aqueous solution

Water soluble PVP capped Au- and Ag-nanoparticles were synthesized and fully characterized.[27] The size of the synthesized spherical Au NPs (15 – 20 nm) and Ag NPs (20 – 40 nm) were established using TEM and DLS analyses. Since the synthesized polymer is insoluble in water, the nanoparticles in water were extracted using chloroform solution of the polymers. We hypothesized that the hydrophobic polyamines interact with nanoparticles at the interface and transfer them to the organic phase through ligand exchange. Extraction experiments were done using initial nanoparticle concentrations of (1.5 mL, 2.5×10^{-4} M) at neutral pH. UV-Vis spectra of Au NP and Ag NP solutions showed absorbance maxima at 510 nm and at 400 nm, respectively. Under normalized conditions, the changes in intensities observed at the absorption maxima after the extractions were used to calculate the extraction capacities of all four copolymers for Au NPs and Ag NPs from water and kinetic data were deduced from the experimental data. The amount of nanoparticles extracted from water to the $CHCl_3$ solution of polyamines was calculated and found to increase with time. The dynamic equilibrium was reached within 20 min, owing to strong interaction of the polymers and nanoparticles (Fig. 5). Control experiments were performed using precursor polymer PS-r-PES (**7**) under similar conditions. The UV absorbance of the NP solutions before and after extractions revealed negligible amounts of NPs were transferred from water to organic phase. This is expected owing to the lack of amine groups on the polymer backbone of precursor polymer, **7**.

Time dependant studies

Figure 5 shows the extraction efficiency of polymers for PVP-coated silver and gold nanoparticles as a function of time. Polymers **P1**, **P2** and **P3** showed equal extraction efficiencies with Q_e values in the range of 30 mg/g and 40 mg/g with respect to Ag NPs and Au NPs, respectively and the extraction was rapid. Polymer with the pyridyl end groups (**P4**) showed lower extraction efficiencies and longer time to reach equilibrium.

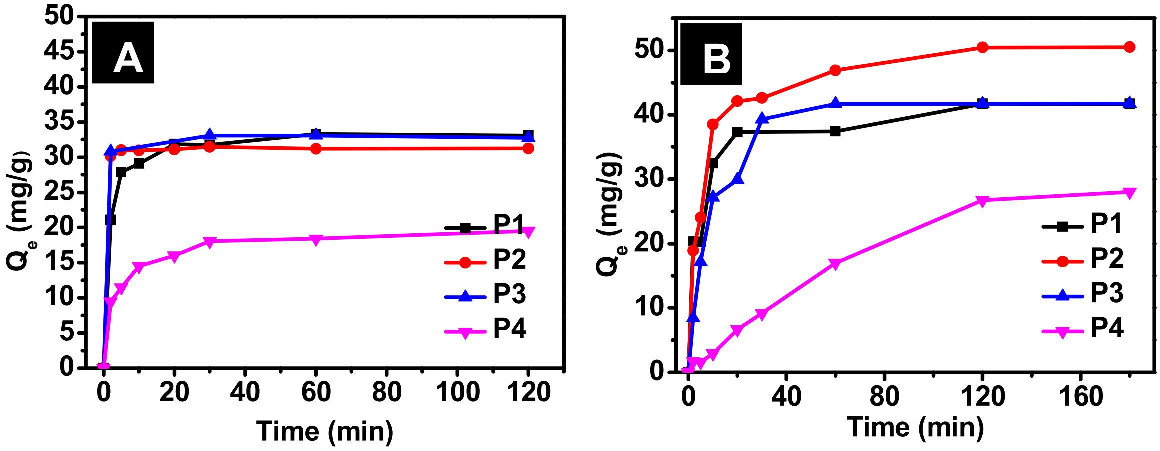

Fig. 5 Effect of contact time on the extraction efficiency of polymers for the extraction of (A) Ag-PVP and (B) Au-PVP from water

Extraction kinetics for metal nanoparticles

The pseudo-first order kinetics plots are given in supplementary information (ESI, Fig. S2). The linear form of pseudo-first order is described as,

$$\log(Q_e\text{-}Q_t) = \log Q_e - (K_1/2.303)t \qquad (2)$$

where, Q_e and Q_t are the amounts of nanoparticles adsorbed at equilibrium (mg/g) and at time ‘t’, respectively; K_1 (min^{-1}) is the rate constant for the pseudo-first order adsorption. From the experimental data, the graph of *log(Q_e-Q_t) versus t* was plotted for all nanoparticles and calculated the pseudo-first order rate constants (ESI, Fig. S2). The R^2 values are significantly lower than 1 indicating poor fit with the pseudo-first order kinetic model, thus pseudo- second order kinetics was applied. The equation for the pseudo-second order kinetics model is given as:

$$t/Q_t = t/Q_e + 1/(K_2.Q_e^2) \qquad (3)$$

where K_2 (g/mg min) is the pseudo-second order rate constant. The values of K_2 and Q_e were calculated from the slope and intercept of the *t/Q_t versus t* plots. Figure 6 shows the graph of the pseudo-second order model for the adsorption of NP’s. Q_e and K_2 values were calculated from the linear graphs and the values are summarised in Table 2. The correlation coefficient in all cases is closer to unity, which signifies that the adsorption follows pseudo-second order model. It is estimated that the electrostatic interactions between the amino groups on the polymer backbone and NPs are responsible for observed extraction efficiencies.[39] The extraction efficiency of pyridyl groups in **P4** is different from aliphatic amine groups on other polymers, which might demonstrate the lower extraction capacity of NPs by **P4**. Similar observations were reported earlier by other research groups.[40,41] However, systematic studies on comparison of extraction efficiencies of pyridine incorporated polymers with other polyamines are not reported. We hypothesize that multiple amine groups on **P1** – **P3** contribute to the extraction of pollutants, while only pyridyl groups are available for coordination for **P4**, which might be the reason for observed low extraction efficiency for polymer **P4**.

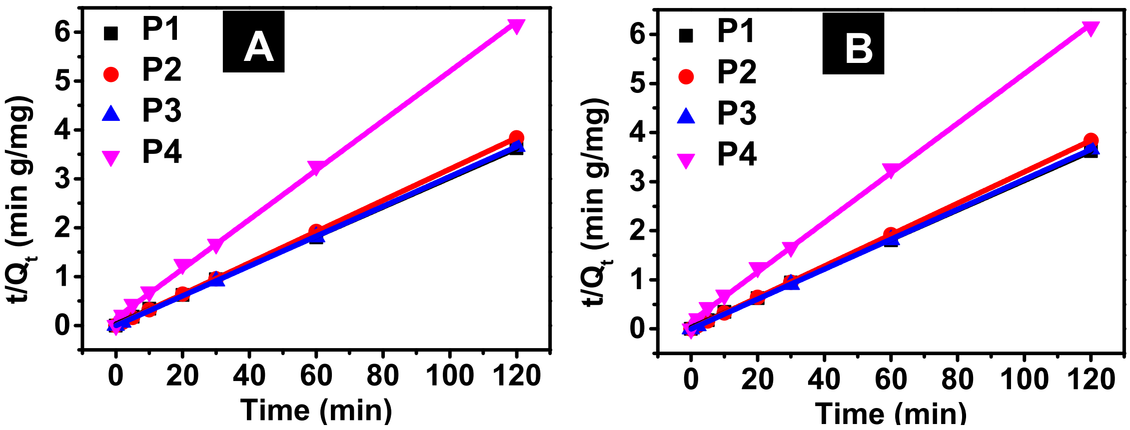

Fig. 6 Pseudo-second order kinetics for the extraction of (A) Ag-PVP and (B) Au-PVP from water using the aminopolymers **P1** – **P4**.

Table 2: Pseudo-second order constants and correlation coefficients for the extraction of NP's using polymers **P1-P4.**

NP's	Polymers	Q_e (exp) (mg/g)	Pseudo-first order kinetic model			Pseudo-second order kinetic model		
			Q_e (mg/g)	K_1 (min^{-1})	R^2	Q_e (mg/g)	K_2 (g/mg min)	R^2
Ag-pvp	**P1**	33.29	8.15	0.0343	0.713	33.40	0.03220	0.999
	P2	31.47	1.56	0.0212	0.158	31.27	0.82477	0.999
	P3	33.08	9.03	0.0279	0.359	32.79	-0.29532	0.999
	P4	19.51	10.68	0.0442	0.794	19.79	0.01730	0.998
Au-pvp	**P1**	41.72	20.58	0.0321	0.509	42.37	0.00738	0.998
	P2	46.10	34.97	0.0184	0.839	51.07	0.00100	0.982
	P3	41.74	32.64	0.0858	0.922	43.48	0.00437	0.997
	P4	28.02	40.49	0.0248	0.948	35.21	0.00055	0.799

Liquid – liquid extraction of dissolved metal ions and dyes from water

Anionic dyes containing sulfonic or carboxylic acid groups are known to adsorb strongly on positively charged adsorbents through electrostatic interactions. Our initial extraction studies showed that cationic dyes such as alcian blue or methylene blue were not significantly extracted by polymers **P1** – **P4** from water. In order to compare the extraction efficiencies of **P1** – **P4** for anionic and neutral dyes, brilliant blue containing sulfonyl groups and neutral red dye with a *tert*-amine group as illustrative dyes were selected. Similarly, aqueous solutions of metal cations (Pb^{2+}) and anions ($Cr_2O_7^{2-}$) were selected for extraction studies. In order to assess the extraction efficiencies of **P1-P4** towards metal ions and organic dyes dissolved in water, stock solutions of polymers dissolved in chloroform (2 mg / mL) were prepared. The polymer solutions (0.5 mL) were mixed with 50 ppm solutions of Brilliant Blue, Neutral red dyes, and heavy metals - lead and chromium ions (1.5 mL each) in separate vials and agitated at 200 rpm at 25 °C and neutral pH. Aqueous samples were then separated from organic fractions at different time intervals of 5, 10, 30, 60, 120, and 240 minutes and each of the samples were analysed by UV absorbance spectrophotometer or ICP-OES analysis for determining the residual dye and metal content. The extraction capacity, Q_e (mg/g) values were calculated using Eqn (1). Figure 7 represents the plots showing the effect of time on the extraction efficiencies towards dyes (A and B) and metal ions (C and D).

It is apparent from the plots that the Q_e values of the four polymers showed higher extraction efficiencies for anionic Brilliant Blue than the neutral red. Based on this data, extraction is strongly dependent on the interactions of positively charged amine groups on the polymer backbone with the negatively charged dyes. Since brilliant blue dyes contain sulfonated (SO_3^-) groups, the protonated amine interact strongly *via* electrostatic interactions. The extraction efficiencies follows the same order in case of brilliant blue and neutral red dyes, i.e., **P4** > **P2** > **P1**.

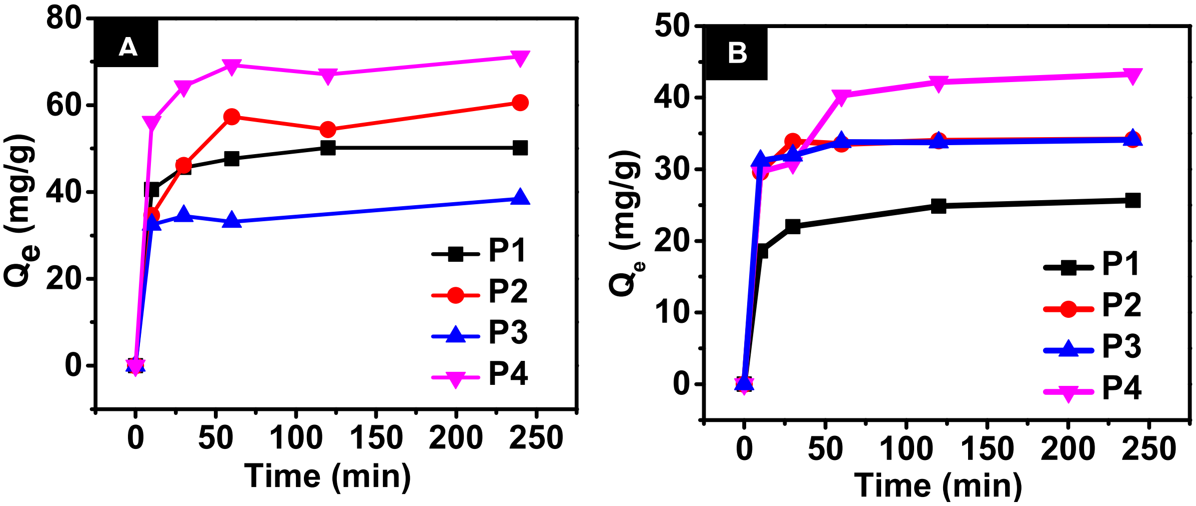

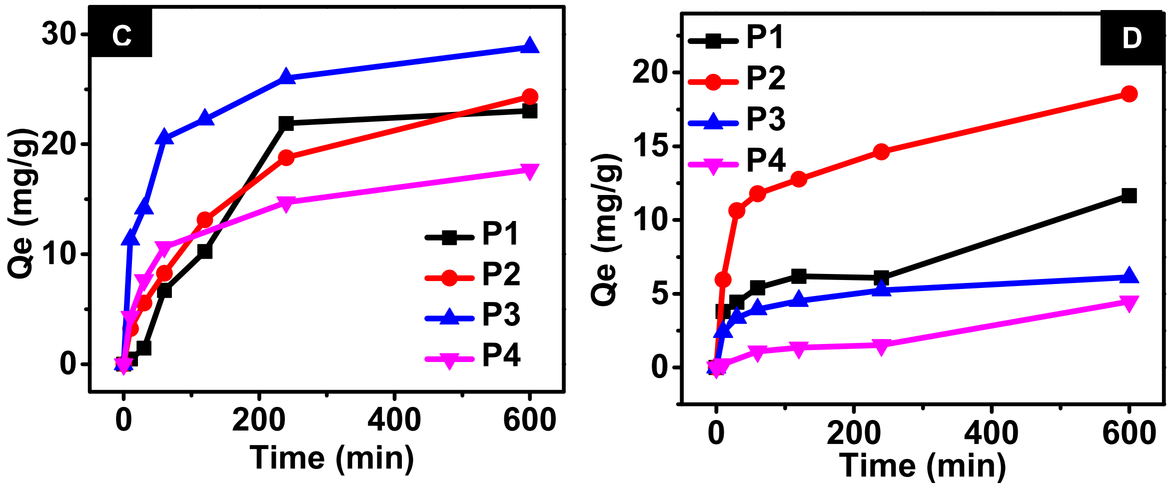

Fig. 7 Effect of contact time on the extraction of (A) brilliant blue, (B) neutral red dyes, (C) lead and (D) chromium ions from water using polymers **P1-P4** at neutral pH.

In the case of metal ions, the extraction efficiency of polymers for Pb(II) ions is higher than hexavalent chromium ions. Cr(VI) ions exist as chromate ($HCrO_4^-$) and dichromate ($Cr_2O_7^{2-}$) ions in solution, the amounts varies with changes in pH of the medium. At neutral pH, the interaction between amine and Cr(VI) anions is lower as compared to solution at acidic pH.[42]

Extraction kinetics for dyes and metal Ions

Pseudo-first order and pseudo-second order kinetics for the adsorption of dyes and metal ions were determined and shown in supporting information (ESI, Fig. S2) and in Figure 8, respectively.

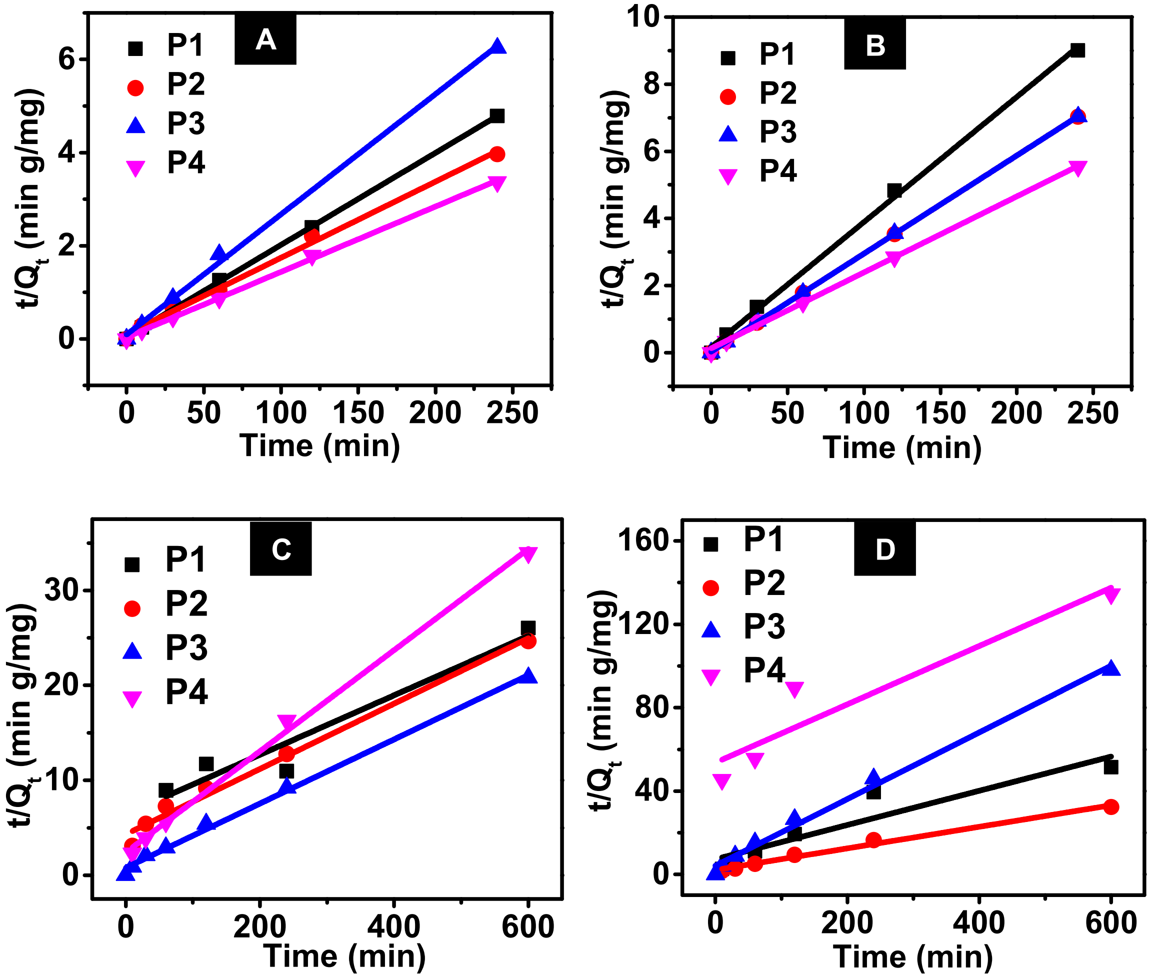

Fig. 8 Pseudo-second order kinetics for (A) brilliant blue, (B) neutral red, (C) lead and (D) chromium ions using polymers **P1** – **P4** in water.

The rate constants, K_1 and K_2 and the Q_e values were calculated from the slope and intercepts of the linear plots and substituting in Eqns (2) and (3). Table 3 summarizes the pseudo-first order and pseudo-second order kinetics data with rate constants (K_1 and K_2) and Qe values. Pseudo-second order kinetics fits better than the pseudo-first order for all polymers as the correlation coefficients (R^2) of pseudo-second order kinetics are closer to unity and the calculated Q_e values match with those determined experimentally.

Adsorption of cationic dyes showed reverse order of adsorption capacity towards different polymers (**P4** > **P2** > **P1**) as compared to the adsorption of NPs. It is known that the amine groups interact with anionic dyes via hydrogen bonding or electrostatic interactions. This trend is linear with increase in number of amine groups on the polymer backbone. **P4** showed lowest extraction efficiency towards chromate anion and NPs.

Interaction of polymers with brilliant blue and neutral red may involve a combination of interactions such as aromatic interactions, *pi-pi*, electrostatic and donor-acceptor interactions involving different groups on the dyes with amine functional groups on the polymer backbone.

Table 3: Pseudo-first order and pseudo-second order constants and correlation coefficients for the extraction of brilliant blue, neutral red dyes and lead and chromium ions by polymers **P1-P4** from water.

Dyes/Metal ions	**Polymers**	**Q_e (exp) (mg/g)**	**Pseudo-first order kinetic model**			**Pseudo-second order kinetic model**		
			Q_e (mg/g)	**K_1 (min^{-1})**	**R^2**	**Q_e (mg/g)**	**K_2 (g/mg min)**	**R^2**
Brilliant Blue	**P1**	50.18	31.3	0.0537	0.9393	50.61	0.00939	0.999
	P2	60.57	30.44	0.0184	0.4575	61.16	0.00253	0.998
	P3	38.42	15.55	0.0271	0.1175	38.73	0.0073	0.997
	P4	71.24	21.98	0.0201	0.3405	71.28	0.00544	0.998
Neutral red	**P1**	26.64	13.18	0.0181	0.6564	26.82	0.00843	0.998
	P2	34.17	6.50	0.0356	0.4811	34.26	0.03706	0.999
	P3	34.21	7.73	0.0321	0.5389	34.21	0.02898	0.999
	P4	43.3	26.24	0.0284	0.8907	44.17	0.004	0.997
Lead	**P1**	23.03	30.10	0.0122	0.889	31.94	0.00015	0.899
	P2	24.32	23.03	0.006	0.996	29.06	0.00027	0.984
	P3	28.82	19.84	0.0085	0.894	29.57	0.00145	0.995

	P4	17.68	13.70	0.0046	0.891	18.77	0.00118	0.996
Chromium	**P1**	11.65	8.43	-0.0021	0.423	12.18	0.00092	0.852
	P2	18.54	4.07	0.0068	0.942	6.25	0.00613	0.991
	P3	6.12	4.13	-0.0016	0.942	7.15	0.00036	0.992
	P4	4.46	4.13	-0.0016	0.730	7.15	0.00036	0.842

Solvent assisted self-organization of polymers

Starting from the pioneering work on the formation of breath figures in polymer films by François *et al,*[43] numerous research groups have studied the effect of moisture and organic solvent on the formation of regular honeycomb structures. Even though, it is now well understood how the casting conditions, such as polymer concentration, humidity and air flow influence the honeycomb structure formation, the role of polymer structure is still ambiguous. The hydrophilic/hydrophobic part of the polymer is expected to play a significant role towards the honeycomb formation.[44] Based on relative fractions of the hydrophobic (styrene) and hydrophilic (amine) groups[45,46] on the polymer backbone, different morphologies may be expected from the self-assembly process. Polymer-solvent interactions and properties of solvents are known to control the packing of polymer chains.[47,48] In the present study, thin films of the copolymers **P1 – P4** were prepared on glass slides by drop-casting polymer solutions (1 mg mL^{-1}) in $CHCl_3$ at room temperature. FESEM was used to establish the morphology of the films formed from different copolymers (Figure 9). Polymer films with porous morphologies were formed by drop-casting $CHCl_3$ solutions of the polymers on glass substrates. Subtle differences in the formation of porous film can be explained owing to the small differences in strucutre of the copolymer backbone.[49-52]

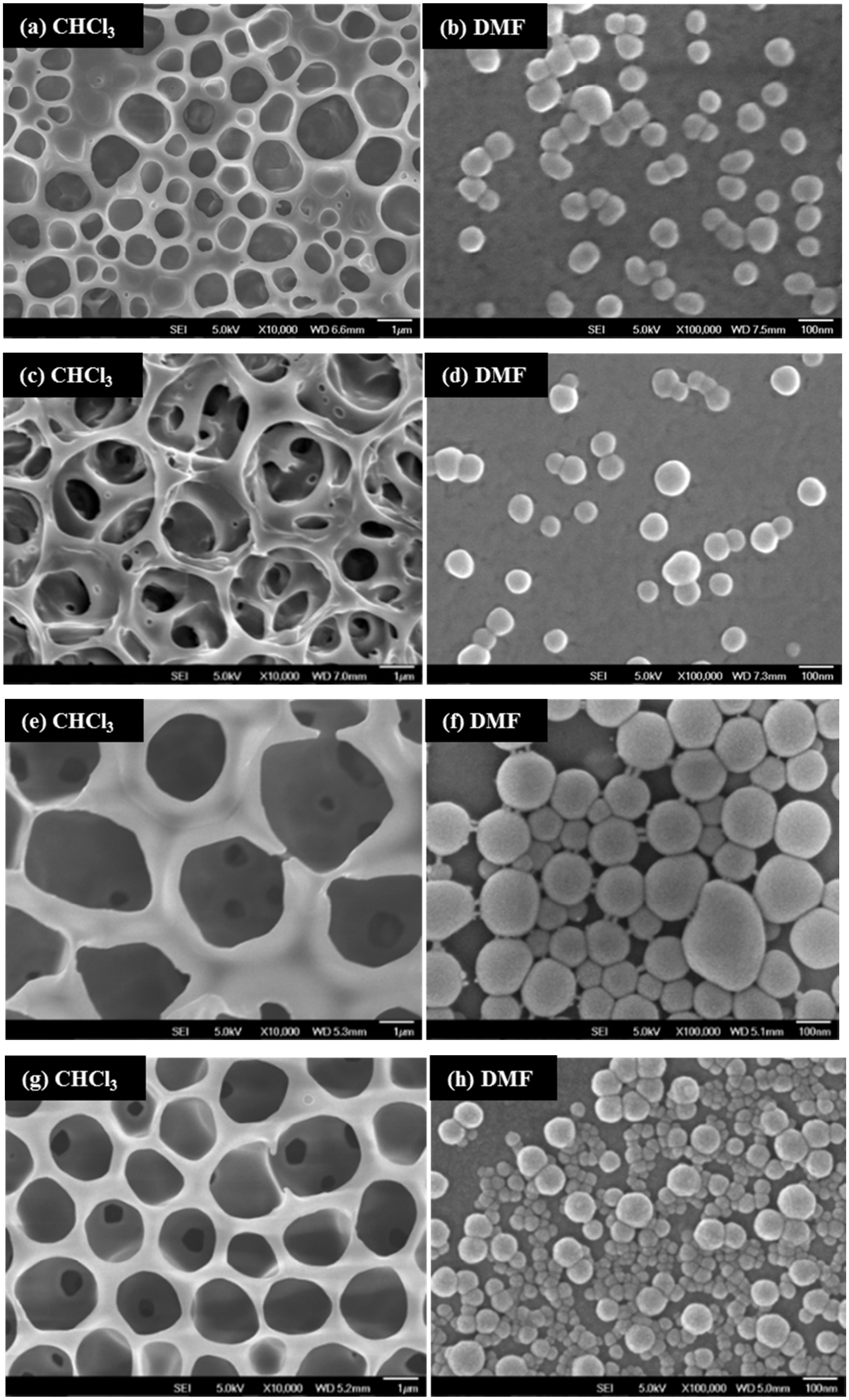
(a) CHCl$_3$
SEI 5.0kV X10,000 WD 6.6mm 1μm
(b) DMF
SEI 5.0kV X100,000 WD 7.5mm 100nm
(c) CHCl$_3$
SEI 5.0kV X10,000 WD 7.0mm 1μm
(d) DMF
SEI 5.0kV X100,000 WD 7.3mm 100nm
(e) CHCl$_3$
SEI 5.0kV X10,000 WD 5.3mm 1μm
(f) DMF
SEI 5.0kV X100,000 WD 5.1mm 100nm
(g) CHCl$_3$
SEI 5.0kV X10,000 WD 5.2mm 1μm
(h) DMF
SEI 5.0kV X100,000 WD 5.0mm 100nm

Fig. 9 SEM images of the morphology of drop-casted film from polymers **P-1** (a-b), **P-2** (c-d), **P-3** (e-f), and **P-4** (g-h) on glass plates from $CHCl_3$ and DMF solutions. Polymer concentration was 1 mg/mL.

Similarly polymer solutions in DMF (1 mg mL^{-1}) were dropcasted on glass plates and allowed the solvent to evaporate under ambient condition. In contrast to the thin films obtained in $CHCl_3$, the polymer solutions in polar, high-boiling solvents such as DMF formed spherical morphologies upon evaporation of solvents.

Solid – liquid Extraction of metal nanoparticles by polymer films

The self-assembled porous films prepared by drop casting the chloroform solution of polymers on glass plates were used for extracting the nanoparticles from water. In this solid-liquid extraction, the polymer film was dipped in aqueous solution of nanoparticles (2 mL) and allowed to stand at room temperature for 3 h. After extraction, the polymer films were imaged by SEM and the micrographs are given in Figure 10.

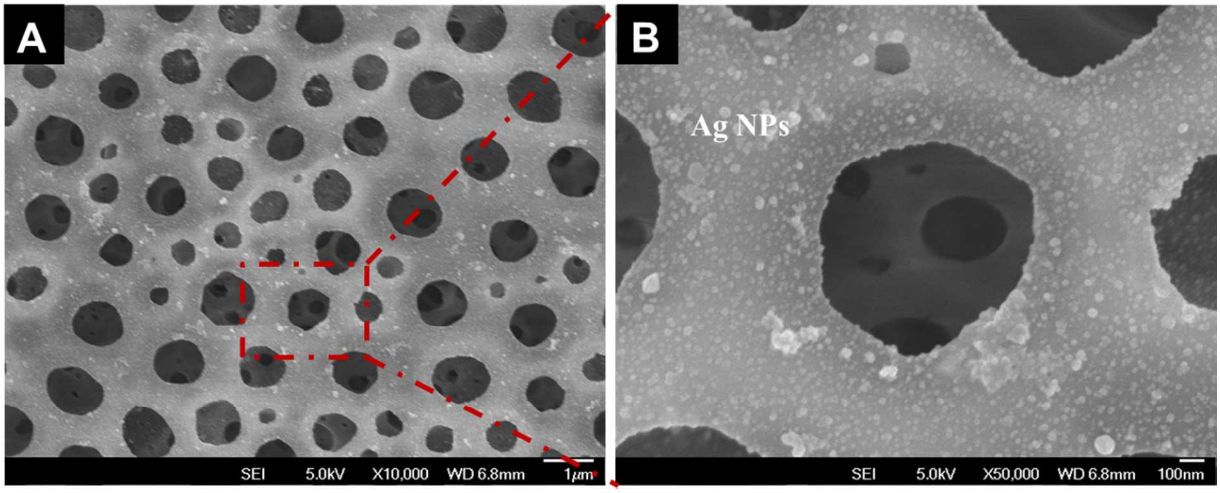

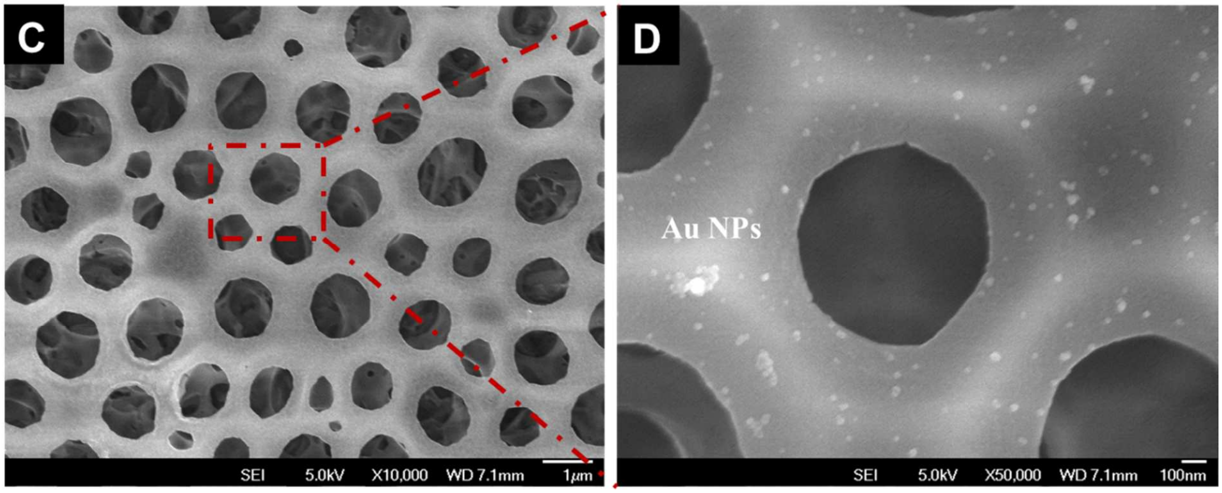

Fig. 10 SEM images of porous film prepared by dropcasting of a chloroform solution of **P1** after extraction of Ag-Cit (A and B) and Au-Cit NPs (C and D).

It is clear that the small white aggregates observed on the surface are metal nanoparticles extracted from solution. However, only amine and triazole groups on the film surface are expected to interact with the hydrophilic nanoparticles in solution, thus the extraction efficiencies of solid films are expected to be lower. We are in the process of optimizing the procedure to quantify solid-liquid extractions and to improve the efficiency by changing the polymer backbone.

Conclusions

In summary, we have successfully synthesized four different polyamines using free radical co-polymerization followed by click reaction as key steps. The convergent method developed to synthesize 1,2,3-triazole ring incorporated polyamines with different spacer lengths from a common alkyne functionalized precursor polymer and corresponding azide derivatives, is versatile and can be extended to prepare a series of polyamines. All polyamines showed porous morphologies after drop casting from hydrophobic chloroform solutions and spherical morphologies from a polar solvent such as DMF. Both liquid – liquid and solid – liquid extractions were performed to establish the affinity of polymers with different pollutants in water. The copolymers were efficient in extracting pollutants such as Ag NPs (33 mg/g), Au NPs (46 mg/g), brilliant blue (60 mg/g), neutral red (34 mg/g) dyes, lead (28 mg/g) and chromium (18 mg/g) ions from water. The amine groups on the polymer backbone and the insolubility of polymers in water are responsible for the observed extraction of pollutants into organic phase. Such readily accessible polyamines may be used for purification of contaminated water.

Acknowledgements

The authors gratefully acknowledge the financial support from the National University of Singapore and Environment and Water Industry Programme Office (EWI) under the National Research Foundation of Singapore (PUBPP 21100/36/2, NUS WBS R-706-002-013-290, R-143-000-458-750, R-143-000-458-731). They also thank the Department of Chemistry, National University of Singapore and NUS Environmental Research Institute (NERI) for all technical support.

Notes and references

*Department of Chemistry, National University of Singapore, 3 Science Drive 3, Singapore 117 543 Correspondence to: S. Valiyaveettil (E - mail: chmsv@nus.edu.sg)

Electronic Supplementary Information (ESI) available: DSC traces for all polymers (Fig. S1) and first-order kinetics data analysis for all extractions using the polymers (Fig. S2).

1. R. Senjen and S.F. Hansen, *C. R. Physique* 2011, **112**, 637–647.

2. S. W. P. Wijnhoven, W. J. G. M. Peijnenburg, C. A. Herberts, W. I. Hagens, A. G. Oomen, E. H. W. Heugens, B. Roszek, J. Bisschops, I. Gosens, D. van de Meent, S. Dekkers, W. H. de Jong, M. van Zijverden, A. J. A. M. Sips and R. E. Geertsma, *Nanotoxicology* 2009, **3**, 109–138.
3. Y. Sag, *Sep. Purif. Method.* 2001, **30**, 1–48.
4. Y. Teow, P. V. Asharani, M. P. Hande and S. Valiyaveettil, *Chem. Commun*. 2011, **47**, 7025–7038.
5. N. Khlebtsov and L. Dykman, *Chem. Soc. Rev.* 2011, **40**, 1647–1671.
6. J. S. Teodoro, A. M. Simões, F. V. Duarte, A. P. Rolo, R. C. Murdoch, S. M. Hussain and C. M. Palmeira, *Toxicol. In Vitro* 2011, **25**, 664–670.
7. E. Frohlich, C. Samberger, T. Kueznik, M. Absenger, E. Roblegg, A. Zimmer and T. R. Pieber, *J. Toxicol. Sci.* 2009, **34**, 363–375.
8. P. V. Asharani, L. W. Yi, Z. Y. Gong and S. Valiyaveettil, *Nanotoxicology* 2011, **5**, 43–54.
9. P. V. Asharani, G. L. K. Mun, M. P. Hande and S. Valiyaveettil, *ACS Nano* 2009, **3**, 279–290.
10. S. Thaiboonrod, C. Berkland, A. H. Milani, R. Ulijn and B. R. Saunders, *Soft Matter* 2013, **9**, 3920–3930.
11. T. O. McDonald, H. Qu, B. R. Saunders and R. V. Ulijn, *Soft Matter* 2009, **5**, 1728–1734.
12. B. Yu, X. Jiang and J. Yin, *Soft Matter* 2011, **7**, 6853–6862
13. X. Chen, H. Lai, C. Xiao, H. Tian, X. Chen, Y. Tao and X. Wang, *Polym. Chem.* 2014, **5**, 6495–6502.

14. R. Bahadur KC, S. R. Bhattarai, S. Aryal, N. Bhattarai, B. M. Lee and H. Y. Kim, *Polym. Int.* 2007, **56**, 518–524.
15. P. Wu, J.-Z. Li, Y.-L. Wang, X.-S. Liu, C. Du, Q.-Y. Tong and N. Li, *Biochem. Eng. J.* 2014, **91**, 66–71.
16. H. Lu, K. Chandran and D. Stensel, *Water Res.* 2014, **64**, 237–254.
17. A. S. Dharnaik and P. K. Ghosh, *Environ. Technol.* 2014, **35**, 2272–2279.
18. R. B. G-Reyes and J. R. Rangel-Mendez, *Bioresour. Technol.* 2010, **101**, 8099–8108.
19. Y.-S. Yun, D. Park, M. J. Park and B. Volesky, *Environ. Sci. Technol. 2001,* ***35****, 4353–4358.*
20. Z. Li, J. Tang and J. Pan, *Food Control* 2004, **15**, 565–570.
21. S. Dalai, S. Pakrashi, M. J. Nirmala, A. Chaudhri, N. Chandrasekaran, A. B. Mandal and A. Mukherjee, *Aquat. Toxicol.* 2013, **138–139**, 1–11.
22. E.-J. Park, J. Yi, Y. Kim, K. Choi and K. Park, *Toxicol. in Vitro*, 2010, **24**, 872–878.
23. S. Deng and Y. P. Ting, *Environ. Sci. Technol.* 2005, **39**, 8490–8496.
24. B. Gao, Y. Li and F. An, *J. Macromol. Sci. Part A Pure Appl. Chem.* 2011, **48**, 823–831.
25. B. Schulze, U. S. Schubert, *Chem. Soc. Rev.* 2014, **43**, 2522–2571.
26. Z. S. Qureshi, R. DSouza, R. Mallampati and S. Valiyaveettil, *J. Appl. Polym. Sci*. 2014, **131**, 40943.
27. R. Mallampati and S. Valiyaveettil, *Nanoscale* 2013, **5**, 3395–3399.
28. K. Tsuda, T. Ishizone, A. Hirao, S. Nakahama, T. Kakuchi and K. Yokota, *Macromolecules* 1993, **26**, 6985–6991.
29. S. Fleischmann, H. Komber and B. Voit, *Macromolecules* 2008, **41**, 5255–5264.
30. R. M. Arnold and J. Locklin, *Langmuir* 2013, **29**, 5920–5926.

31. R. K. O-Reilly, M. J. Joralemon, C. J. Hawker and K. L. Wooley, *Chem. Eur. J.* 2006, **12**, 6776–6786.

32. M. Malkoch, R. J. Thibault, E. Drockenmuller, M. Messerschmidt, B. Voit, T. P. Russell, and C. J. Hawker, *J. Am. Chem. Soc.* 2005, **127**, 14942–14949.

33. M. Ramakrishna and S. Valiyaveettil, *RSC Adv.* 2012, **2**, 9914–9920.

34. R. K. Iha, K. L. Wooley, A. M. Nyström, D. J. Burke, M. J. Kade and C. J. Hawker, *Chem. Rev.* 2009**, 109***,* 5620–5686.

35. H. Durmaz, A. Sanyal, G. Hizal and U. Tunca, *Polym. Chem.* 2012, **3**, 825–835.

36. A. Qin, J. W. Y. Lam and B. Z. Tang, *Chem. Soc. Rev.* 2010, **39**, 2522–2544.

37. R. Farley and B. R. Saunders, *Polymer* 2014, **55**, 471–480.

38. P. Yang, L. Wang, R. Feng, A. A. Almehizia, Q. Tong, K-Z. Myint, Q. Ouyang, M. H. Alqarni, L. Wang and X-Q. Xie, *J. Med. Chem.* 2013, **56**, 2045–2058.

39. Y. Yuan, D. Ding, K. Li, J. Liu and B. Liu, *Small* 2014, **10**, 1967–1975.

40. Kim, K.; Ryoo, H.; Shin, K. S. *Langmuir* 2010, **26**, 10827-10832.

41. Ryoo, H.; Kim, K.; Shin, K. S. *Vibrational Spectroscopy* 2010, **53**, 158-162.

42. R. Cheng, S. Ou, B. Xiang, Y. Li and Q. Liao, *J. Polymer Research* 2009, **16**, 703–708.

43. G. Widawski, M. Rawiso and B. François, *Nature* 1994, **369**, 387–389.

44. V. D. Deepak and S. K. Asha, *J. Polym. Sci., Part A: Polym. Chem.* 2008, **46**, 1278–1288.

45. S. Jain and F. S. Bates, *Science* 2003, **300**, 460–464.

46. S. Jain and F. S. Bates, *Macromolecules* 2004, **37**, 1511–1523.

47. T. P. Lodge, B. Pudil and K. J. Hanley, *Macromolecules* 2002, **35**, 4707–4717.

48. M. J. Park, K. Char, J. Bang and T. P. Lodge, *Macromolecules* 2005, **38**, 2449–2459.

49. M. H. Nurmawati, R. Renu, P. K. Ajikumar, S. Sindhu, F. C. Cheong, C. H. Sow and S. Valiyaveettil, *Adv. Funct. Mater*. 2006, **16**, 2340–2345.
50. Z. S. Guo, J. Pei, Z. L. Zhou, L. Zhao, G. Gibson, S. Lam and J. Brug, *Polymer* 2009, **50**, 4794–4800.
51. V. D. Deepak and S. K. Asha, *J. Phys. Chem. B* 2006, **110**, 21450–21459.
52. Y. Dianjun, T. Bindu and R. S. Pudupadi, *Macromolecules* 2006, **39**, 7786–7788.